# Solar neutrinos: Global analysis with day and night spectra from SNO

Pedro C. de Holanda
*The Abdus Salam International Centre for Theoretical Physics, I-34100 Trieste, Italy*

A. Yu. Smirnov
*The Abdus Salam International Centre for Theoretical Physics, I-34100 Trieste, Italy*
*and Institute for Nuclear Research of Russian Academy of Sciences, Moscow 117312, Russia*
(Received 22 July 2002; published 27 December 2002)

We perform global analysis of the solar neutrino data including the day and night spectra of events at SNO. In the context of two active neutrino mixing, the best fit of the data is provided by the large-mixing angle (LMA) Mikheyev-Smirnov-Wolfenstein solution with $\Delta m^2 = 6.15\times 10^{-5}$ eV$^2$, $\tan^2\theta = 0.41$, $f_B = 1.05$, where $f_B$ is the boron neutrino flux in units of the corresponding flux in the standard solar model (SSM). At the $3\sigma$ level we find the following upper bounds: $\tan^2\theta < 0.84$ and $\Delta m^2 < 3.6\times 10^{-4}$ eV$^2$. From a $1\sigma$ interval we expect the day-night asymmetries of the charged current and electron scattering events to be $A_{\rm DN}^{\rm CC} = 3.9^{+3.6}_{-2.9}\%$ and $A_{\rm DN}^{\rm ES} = 2.1^{+2.1}_{-1.4}\%$. The only other solution which appears at the $3\sigma$ level is the VAC solution with $\Delta m^2 = 4.5\times 10^{-10}$ eV$^2$, $\tan^2\theta = 2.1$, and $f_B = 0.75$. The best fit point in the low probability, low mass region, with $\Delta m^2 = 0.93\times 10^{-7}$ eV$^2$ and $\tan^2\theta = 0.64$, is accepted at 99.95% ($3.5\sigma$) C.L. The least $\chi^2$ point from the small mixing angle solution region, with $\Delta m^2 = 4.6\times 10^{-6}$ eV$^2$ and $\tan^2\theta = 5\times 10^{-4}$, could be accepted at the $5.5\sigma$ level only. In the three neutrino context the influence of $\theta_{13}$ is studied. We find that with an increase of $\theta_{13}$ the LMA best fit point shifts to a larger $\Delta m^2$, the mixing angle is practically unchanged, and the quality of the fit becomes worse. The fits of LOW and SMA slightly improve. Predictions for the KamLAND experiment (total rates, spectrum distortion) have been calculated.

DOI: 10.1103/PhysRevD.66.113005 PACS number(s): 26.65.+t, 14.60.Lm, 14.60.Pq, 95.85.Ry

## I. INTRODUCTION

The SNO data [1–5] is the breakthrough in the long story of the solar neutrino problem. With a high confidence level we can claim that solar neutrinos undergo the flavor conversion

$$\nu_e \to \nu_\mu, \nu_\tau \quad \text{or/and} \quad \bar{\nu}_\mu, \bar{\nu}_\tau. \tag{1}$$

Moreover, nonelectron neutrinos compose a larger part of the solar neutrino flux at high energies (also partial conversion to sterile neutrinos is not excluded). The main issue now is to identify the *mechanism* of neutrino conversion.

There are several important pieces of new information from the recent SNO publication [3–5].

(1) Measurements of the energy spectra with low threshold (as well as angular distribution) of events allow one to extract information on the neutrino neutral current (NC), charged current (CC), as well as electron scattering (ES) event rates. In particular, in assumption of absence of distortion, one gets for the ratio of the NC/CC event rates:

$$\frac{\rm NC}{\rm CC} = 2.9 \pm 0.4 \tag{2}$$

which deviates from 1 by about $5\sigma$.

(2) Measurements of the day and night energy spectra allow one to find the D-N asymmetries of different classes of events. Under constraint that total flux has no D-N asymmetry one gets for the CC event rate [4]

$$A_{\rm DN}^{\rm CC} = 7.0 \pm 4.9^{+1.5}_{-1.4}\%. \tag{3}$$

(3) No substantial distortion of the neutrino energy spectrum has been found.

(4) Solutions of the solar neutrino problem based on pure active–sterile conversion, $\nu_e \to \nu_s$, are strongly disfavored.

These results further confirm earlier indications of $\nu_\mu -, \nu_\tau -$ appearance from comparison of fluxes determined from the charged current event rate in the SNO detector [1,2], and the $\nu e -$ scattering event rate obtained by the Super-Kamiokande (SK) collaboration [6–8].

Implications of the new SNO results for different solutions (see [9,10] for earlier studies) can be obtained immediately by comparison of the results (2, 3) with predictions from the best fit points of different solutions [11–17]. In particular, for the large mixing angle (LMA) solution the best fit prediction NC/CC = 3.3 (for lower threshold) [15] is slightly higher than Eq. (2). So, new results should move the best fit point to larger values of mixing angles. The expected day–night asymmetry in the best fit point, $\sim 6\%$, is well within the interval (3). Clearly new data further favor this solution.

For low probability, low mass (LOW) solution: NC/CC = 2.4 [15] in the best fit point, which is $1\sigma$ (experimental) lower than the central SNO value. The expected asymmetry was lower than Eq. (3), therefore this solution is somewhat less favored, and SNO tends to shift the allowed region to smaller values of $\theta$ which correspond to smaller survival probability.

Implications of new SNO results have been studied in [18–22]. In this paper we continue this study. We perform global analysis of all available data including the SNO day and night energy spectra of events, and the latest data from

 

Super-Kamiokande and SAGE. We identify the most plausible solutions and study their properties.

The paper is organized as follows: In Sec. II we describe features of our analysis. In Sec. III we present results of the $\chi^2$ test and construct the pull-off diagrams for various observables. In Sec. IV we determine the regions of solutions and describe their properties. In Sec. V we consider the effect of $\theta_{13}$ on the solutions. In Sec. VI we study the predictions to KamLAND for the parameters given by the found solutions. The conclusion is given in Sec. VII.

## II. GLOBAL ANALYSIS OF THE SOLAR NEUTRINO DATA

In this section we describe the main ingredients of our analysis. We follow the procedure of analysis developed in previous publications [9,10,15,16,23].

### A. Input data

We use the following set of the experimental results:

(1) Three rates (3 degrees of freedom):

(i) the Ar production rate $Q_{\rm Ar}$ measured by the Homestake experiment [24],

(ii) the Ge production rate, $Q_{\rm Ge}$, from SAGE [25],

(iii) the combined Ge production rate from GALLEX and GNO [26].

(2) The zenith-spectra measured by Super-Kamiokande [6] during 1496 days of operation. The data consists of eight energy bins with seven zenith angle bins in each, except for the first and last energy bins, which makes 44 data points. We use the experimental errors given in [7] and we treat the correlation of systematic uncertainties as in [16]. Following the procedure outlined in [10] we do not include the total rate of events in the SK detector, which is not independent from the spectral data.

(3) From SNO, we use the day and the night energy spectra of all events [5]. We follow procedure described in [5]. Additional information on how to treat the systematic uncertainties was given by [27].

Altogether there are 81 data points.

### B. Neutrino fluxes

All solar neutrino fluxes (but the boron neutrino flux) are taken according to standard solar model (SSM) of Bahcall, Pinsonneault, and Basu (BPB2000) [28]. We use the boron neutrino flux as a free parameter. We define dimensionless parameter

$$f_B \equiv \frac{F_B}{F_B^{\rm SSM}}, \tag{4}$$

where the SSM boron neutrino flux is taken to be $F_B^{\rm SSM} = 5.05\times 10^6\ {\rm cm}^{-2}\ {\rm s}^{-1}$. For the *hep* neutrino flux we take fixed value $F_{hep} = 9.3\times 10^3\ {\rm cm}^{-2}\ {\rm s}^{-1}$ [28,29].

### C. Neutrino mixing and conversion

We perform analysis of data in terms of mixing of two flavor neutrinos and three flavor neutrinos.

In the case of two neutrinos there are two oscillation parameters: the mass squared difference, $\Delta m^2$, and the mixing parameter $\tan^2\theta$. So, we have three fit parameters: $\Delta m^2$, $\tan^2\theta$, $f_B$, and therefore 81 (data points) $-3 = 78$ degrees of freedom (DOF).

In the case of three neutrino mixing we adopt the mass scheme which explains the solar and the atmospheric neutrino data. In this scheme the mass eigenstates $\nu_1$ and $\nu_2$ are splitted by the solar $\Delta m^2_{12}$, whereas the third mass eigenstate, $\nu_3$, is separated by larger mass split related to the atmospheric $\Delta m^2_{13}$. Matter effect influences very weakly mixing (flavor content) of the third mass eigenstate. The effect of third neutrino is reduced then to the averaged vacuum oscillations. In this case, the survival probability equals

$$P_{ee} = \cos^4\theta_{13} P_{ee}^{(2)} + \sin^4\theta_{13}, \tag{5}$$

where $\sin\theta_{13} \equiv U_{e3}$ describes the mixing of electron neutrino in the third mass eigenstate and $P_{ee}^{(2)}$ is the two neutrino oscillation probability characterized by $\tan^2\theta_{12}$, $\Delta m^2_{12}$ and the effective matter potential reduced by factor $\cos^2\theta_{13}$ (see e.g., [30,31] for previous studies).

In general, in the three neutrino case the fit parameters are $\tan^2\theta_{12}$, $\Delta m^2_{12}$, $\sin\theta_{13}$, and $f_B$. However, here for illustrative purpose we take the fixed value of $\theta_{13}$ near its upper bound. So, the number of degrees of freedom is the same as in the two neutrino case.

### D. Statistical analysis

We perform the $\chi^2$ test of various oscillation solutions by calculating

$$\chi^2_{\rm global} = \chi^2_{\rm rate} + \chi^2_{\rm SK} + \chi^2_{\rm SNO}, \tag{6}$$

where $\chi^2_{\rm rate}$, $\chi^2_{\rm SK}$, and $\chi^2_{\rm SNO}$ are the contributions from the total rates, from the Super-Kamiokande zenith spectra, and the SNO day and night spectra correspondingly. Each of the entries in Eq. (6) is the function of three parameters ($\Delta m^2$, $\tan^2\theta$, $f_B$).

Some details of treatment of the systematic errors are given in the Appendix.

The uncertainties of contributions from different components of the solar neutrino flux (*pp*-, Be-, B-, etc.) to Ge-production rate due to uncertainties of the cross section of the detection reaction $\nu_e - {\rm Ga}$ correlate. Similarly, uncertainties of contributions to Ar production rate due to uncertainty in $\nu_e - {\rm Cl}$ cross section correlate. Following [32] we have taken into account these correlations.

### E. Cross-checks. Comparison with other analysis

We have checked our results performing two additional fits:

(1) To check our treatment of the SK data we have performed global analysis taking from SNO only the CC rate. That corresponds to the analysis done in [7,8]. We get very good agreement of the results.

(2) To check our treatment of the latest SNO data we have performed analysis using the day and night spectra from

TABLE I. Best-fit values of the parameters $\Delta m^2$, $\tan^2\theta$, and $f_B$, as well as the minimum $\chi^2$ and the corresponding goodness of fit (g.o.f.) for various global solutions. The number of degrees of freedom is 78.

| Solution | $\Delta m^2/\mathrm{eV}^2$ | $\tan^2\theta$ | $f_B$ | $\chi^2_{\min}$ | g.o.f. |
|---|---|---|---|---|---|
| LMA | $6.15\times10^{-5}$ | 0.41 | 1.05 | 65.2 | 85% |
| VAC | $4.5\times10^{-10}$ | 2.1 | 0.749 | 74.9 | 58% |
| LOW | $0.93\times10^{-7}$ | 0.64 | 0.908 | 77.6 | 49% |
| SMA | $4.6\times10^{-6}$ | $0.5\times10^{-3}$ | 0.57 | 99.7 | 4.9% |

SNO, as in [4]. We have reproduced the results of paper [4] with good accuracy.

Our input set of the data differs from that used in other analyses: We include more complete and up-dated information. SNO [4] uses the SK day and night spectra measured after 1258 days. In contrast, we use preliminary SK zenith spectra measured during 1496 days. In [19] the NC/CC ratio and the D-N asymmetry at SNO where included in the analysis. The analysis done by Barger *et al.* [18] uses the same data set we do.

## III. $\chi^2$ TEST

In this section we describe the results of fit for two neutrino mixing.

In Table I we show the best fit values of parameters $\Delta m^2$, $\tan^2\theta$, $f_B$ for different solutions of the solar neutrino problem. We also give the corresponding values of $\chi^2_{\min}$ and the goodness of the fit.

The absolute $\chi^2$ minimum, $\chi^2=65.2$ for 78 DOF, is in the LMA region. The vacuum oscillation is the next best. It, however, requires $\sim$30% lower boron neutrino flux. The LOW solution has slightly higher $\chi^2$. The small mixing angle (SMA) gives a very bad fit.

In order to check the quality of the fits we have calculated predictions for the available observables in the best fit points of the global solutions (see Table I). Using these predictions we have constructed the ''pull-off'' diagrams (Fig. 1) which show deviations, $D_K$, of the predicted values of observables $K$ from the central experimental values expressed in the $1\sigma$ unit:

$$D_K \equiv \frac{K_{bf}-K_{\exp}}{\sigma_K},$$

$$K \equiv Q_{\mathrm{Ar}},\quad Q_{\mathrm{Ge}},\quad \mathrm{NC/CC},\quad R_{\nu e},\quad A^{\mathrm{SK}}_{\mathrm{DN}}, A^{\mathrm{CC}}_{\mathrm{DN}}. \tag{7}$$

Here $\sigma_K$ is the one sigma standard deviation for a given observable $K$. $R_{\nu e}$ is the reduced total rate of events at SK. We take the experimental errors only: $\sigma_K=\sigma_K^{\exp}$.

According to Fig. 1 only the LMA solution does not have strong deviations of predictions from the experimental results. LOW and VAC solutions give worse fit to the data.

## IV. PARAMETERS OF SOLUTIONS

We define the solution regions by constructing the contours of constant (68%, 90%, 95%, 99%, 99.73%) confidence level with respect of the absolute minimum in the LMA region. Following the same procedure as in [10], for each point in the $\Delta m^2$, $\tan^2\theta$ plane we find minimal value $\chi^2_{\min}(\Delta m^2,\tan^2\theta)$ varying $f_B$. We define the contours of constant confidence level by the condition

$$\chi^2_{\min}(\Delta m^2,\tan^2\theta)=\chi^2_{\min}(\mathrm{LMA})+\Delta\chi^2, \tag{8}$$

where $\chi^2_{\min}$ (LMA)$=65.2$ is the absolute minimum in the LMA region and $\Delta\chi^2$ is taken for two degrees of freedom.

### A. LMA

Recent SNO data further favors the LMA Mikheyev-Smirnov-Wolfenstein (MSW) solution (see, e.g., [33]). In the best fit point we get

$$\Delta m^2=6.15\times10^{-5}\ \mathrm{eV}^2,\quad \tan^2\theta=0.41,\quad f_B=1.05. \tag{9}$$

The value of $\Delta m^2$ is slightly higher than that found in the SNO analysis and higher than in our previous analysis [15]. The shift is mainly due to updated SK results which show smaller D-N asymmetry than before. Large SNO asymmetry which would push $\Delta m^2$ to smaller values is still statistically insignificant. The mixing angle is shifted to larger values (in comparison with previous analysis) due to smaller ratio of the NC/CC event rates. The boron neutrino flux is 5% higher

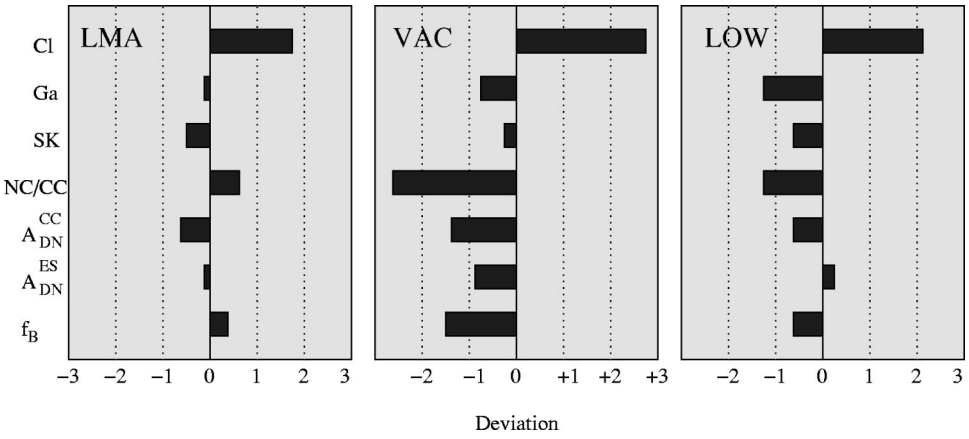


FIG. 1. Pull-off diagrams for global solutions. Shown are deviations of predictions from experimentally measured values for the Ar-production rate, Ge-production rate, SK rate, the day-night asymmetries at SK and SNO. The pull-offs are expressed in the units of 1 standard deviation, $1\sigma$.

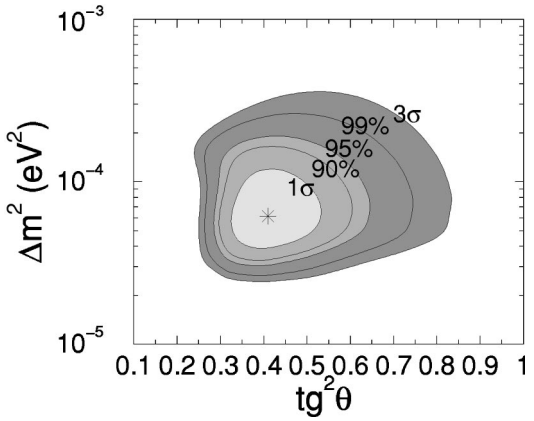


FIG. 2. The global LMA MSW solution. The boron neutrino flux is considered as a free parameter. The best fit point is marked by a star. The allowed regions are shown at $1\sigma$, 90% C.L., 95% C.L., 99% C.L., and $3\sigma$.

than the central value in the SSM: $F_B = f_B \cdot F_B^{\rm SSM} = 5.32 \times 10^6$ cm$^{-2}$ s$^{-1}$ being, however, within $1\sigma$ deviation and well in agreement with SNO measurements.

The C.L. contours (see Fig. 2) shrink substantially as compared with previous determination [11–17].

From Fig. 2 we find the following bounds on oscillations parameters.

(1) $\Delta m^2$ is rather sharply restricted from below by the day–night asymmetry at SK: $\Delta m^2 > 2.3 \times 10^{-5}$ eV$^2$ at 99.73% C.L.

(2) The upper limits on $\Delta m^2$ for different confidence levels equal:

$$\Delta m^2 \leqslant \begin{cases} 1.2\times 10^{-4} \text{ eV}^2, & 68.27\% \text{ C.L.}, \\ 1.9\times 10^{-4} \text{ eV}^2, & 95\% \text{ C.L.}, \\ 3.6\times 10^{-4} \text{ eV}^2, & 99.73\% \text{ C.L.} \end{cases} \tag{10}$$

All these limits are stronger than the CHOOZ [34] bound which appears for maximal mixing at $\Delta m^2 \sim 8 \times 10^{-4}$ eV$^2$.

(3) The upper limit on mixing angle becomes substantially stronger than before:

$$\tan^2\theta < \begin{cases} 0.53, & 68.27\% \text{ C.L.}, \\ 0.65, & 95\% \text{ C.L.}, \\ 0.84, & 99.73\% \text{ C.L.} \end{cases} \tag{11}$$

Maximal mixing is allowed at the $\sim 4\sigma$ level for $\Delta m^2 = (5-7) \times 10^{-5}$ eV$^2$.

Notice that the SNO data alone exclude maximal mixing at about $3\sigma$: the data determine now rather precisely the NC/CC ratio which is directly related to $\sin^2\theta$. Also observed germanium production rate as well as argon production rate disfavor maximal mixing [see Figs. 3(a) and 3(b)].

So, now we have strong evidence that solar neutrino mixing significantly deviates from maximal value. One can introduce the deviation parameter [35]

$$\epsilon \equiv 1 - 2\sin^2\theta. \tag{12}$$

From our analysis we get

$$\epsilon > 0.08 \quad (3\sigma). \tag{13}$$

That is, at $3\sigma$: $\epsilon > \sin^2\theta_c$, where $\theta_c$ is the Cabibbo angle. This result has important theoretical implications.

(4) *Lower* limit on mixing:

$$\tan^2\theta > 0.23, \quad 99\% \text{ C.L.} \tag{14}$$

is changed weakly.

In Figs. 3(a)–3(d) we show the grids of predicted values for various observables.

According to the pull-off diagram and Figs. 3(a)–3(d), the LMA solution reproduces observables at $\sim 1\sigma$ or better. The largest deviation is for the Ar production rate: the solution predicts a $1.6\sigma$ larger rate than the Homestake result.

The best fit point value and $3\sigma$ interval for Ge production rate equal

$$Q_{\rm Ge} = 70.5 \text{ SNU}, \quad Q_{\rm Ge} = (63-84) \text{ SNU}, \quad 3\sigma. \tag{15}$$

Notice that at maximal mixing $Q_{\rm Ge} < 63$ SNU which is $2\sigma$ away from the combined experimental result.

### B. VAC

In the best fit point we get $\chi^2 = 74.9$ and

$$\chi^2(\text{VAC}) - \chi^2(\text{LMA}) = 9.7. \tag{16}$$

So, this solution is accepted at the $3\sigma$ level. Notice that the solution appears in the dark side of the parameter space which means that some matter effect is present. This solution was ''discovered'' in 1998 and its properties have already been described in the literature. Clearly it does not predict any day–night asymmetry. The solution requires rather low ($1.6\sigma$) boron neutrino flux and gives rather poor description of rates (see Fig. 1). In particular, a $2.7\sigma$ higher Ar production rate and a $2.6\sigma$ lower NC/CC ratio are predicted. Imposing the SSM restriction on this flux leads to exclusion of this VAC solution at the $3\sigma$ level.

### C. Any chance for SMA?

We find that the best fit point from the SMA region has $\chi^2 = 99.8$. For the difference of $\chi^2$ we have:

$$\chi^2(\text{SMA}) - \chi^2(\text{LMA}) = 34.5. \tag{17}$$

That is, SMA is accepted at $5.5\sigma$ only. Moreover, the solution requires about $3\sigma$ lower boron neutrino flux than in the SSM. It predicts negative day–night asymmetry: $A_{\rm DN}^{\rm CC} = -0.93\%$.

Our results are in qualitative agreement with those in [18], where even larger $\Delta\chi^2$ has been obtained.

We find that the $\chi^2$ increases weakly with $\tan^2\theta$ up to $\tan^2\theta = 1.5 \times 10^{-3}$, where $\chi^2 \sim 105$.

Is SMA excluded? We find that very bad fit is due to the latest SNO measurements of day and night spectra. We have checked that the analysis of the same set of data but CC rate

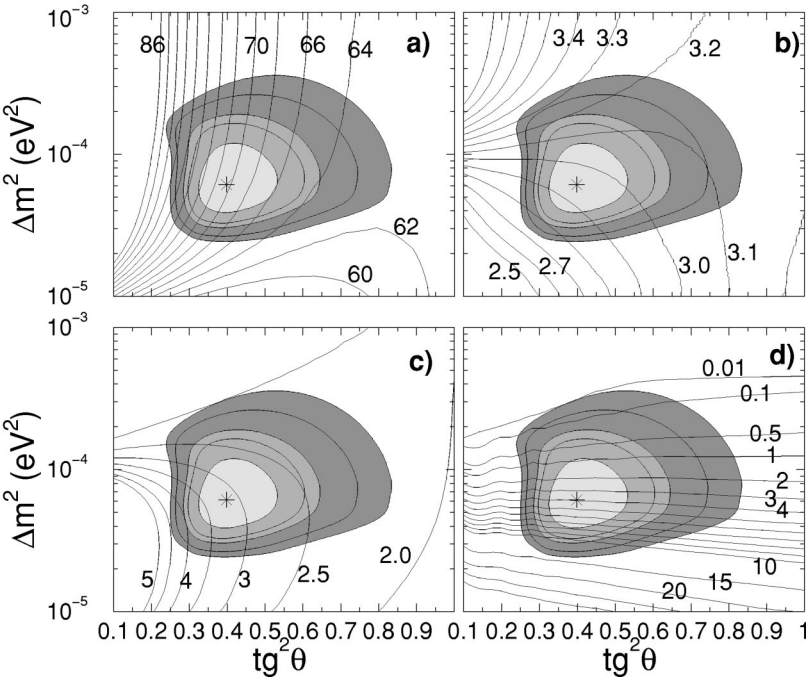


FIG. 3. Lines of constant (a) Ge production rate, (b) Ar production rates (number at the curves in SNU), (c) NC/CC ratio, and (d) day–night asymmetry of CC events in the LMA region. In the best fit point: $R_{\mathrm{Ge}}=70.5$ SNU, $R_{\mathrm{Ar}}=2.95$ SNU, NC/CC$=3.15$, and $A_{\mathrm{DN}}^{\mathrm{CC}}=3.9\%$. The dependence of $f_B$ on oscillation parameters is taken into account.

from SNO only (2001 year) instead of spectrum leads to the best fit values $\Delta m^2=4.8\times10^{-6}$ eV$^2$, $\tan^2\theta=3.9\times10^{-4}$, and $f_B=$ and $\chi^2(\mathrm{SMA})-\chi^2(\mathrm{LMA})=11$ in good agreement with results of a similar analysis in [8]. Since CC SNO data are in a good agreement with the new NC/CC result, just using the NC/CC does not produce a substantial change of quality of the SMA fit [19]. So it is the spectral data which give a large contribution to $\chi^2$.

The SMA solution with very small mixing provides rather good description of the SK data: the rate and spectra. The (reduced) rate $R\equiv$OBS/SSM of the ES events can be written as

$$[\mathrm{ES}]=f_B[P_{ee}(1-r)+r], \tag{18}$$

where $r\approx0.16$ is the ratio of $\nu_\mu-e$ to $\nu_e-e$ cross sections. Taking $R_{\mathrm{ES}}=0.45$ and $f_B=0.58$ we find the effective survival probability: $P_{ee}=0.73$. Then, for reduced CC event rate we get $[\mathrm{CC}]=f_BP_{ee}=0.425$, close to the ES rate, and moreover,

$$\mathrm{NC/CC}\approx1/P_{ee}=1.37, \tag{19}$$

which is substantially smaller then the observed quantity (2). So, one predicts in this case a suppressed contribution of the NC events to the total rates. Correspondingly, significant distortion of the energy spectrum of events is expected with a smaller than observed rate at low energies and a higher rate at high energies.

This problem with SNO could be avoided for larger mixing: $\tan^2\theta>1.5\times10^{-3}$ (in fact, imposing the SSM restriction on the boron neutrino flux leads to the shift of the best fit point to larger $\theta$). In this case, however, serious problems with SK data appear, namely, with spectrum distortion and zenith angle distribution. Strong day–night asymmetry is predicted for the Earth core-crossing bin. Previous analysis which used SK day and night spectra could not realize the latter problem.

Notice that the SNO data alone do not disfavor SMA with large $\tan^2\theta=(1.5\text{–}2)\times10^{-3}$. This region, however, is strongly disfavored by SK.

Zenith angle distribution can give a decisive check of the SMA solution. The SNO night data could be divided into two bins: ''mantle'' and ''core.'' Concentration of the night excess of rate in the core bin [36] due to parametric enhancement of oscillations for the core crossing trajectories [37], would be the evidence of the SMA solution with relatively large mixing: $\tan^2\theta=(1.5\text{–}2)\times10^{-3}$. However, the SK zenith spectra do not show any excess of the ''core'' bin rate which testify against this possibility.

Probably some unknown systematics could improve the SMA fit. Otherwise, this solution is practically excluded.

### D. LOW starts to disappear?

In the best fit point we get $\chi^2=78.9$, so that

$$\chi^2(\mathrm{LOW})-\chi^2(\mathrm{LMA})=12.4, \tag{20}$$

which is slightly beyond the $3\sigma$ range. In contrast with other analyses, LOW does not appear at the $3\sigma$ level. Notice that in the SNO analysis [4] the LOW solution exists marginally at the $3\sigma$ level. Inclusion of the SK data which contain information about zenith angle distribution (zenith spectra) worsen the fit (this effect has also been observed in [13]).

The LOW solution gives rather poor fit of total rates. In the best fit point we get $2.1\sigma$ larger Ar production rate and $1.2\sigma$ lower Ge production rate. For the day–night asymmetry of the CC events we predict $A_{\mathrm{DN}}^{\mathrm{CC}}=3.5\%$ and for ES events: $A_{\mathrm{DN}}^{\mathrm{CC}}=2.7\%$.

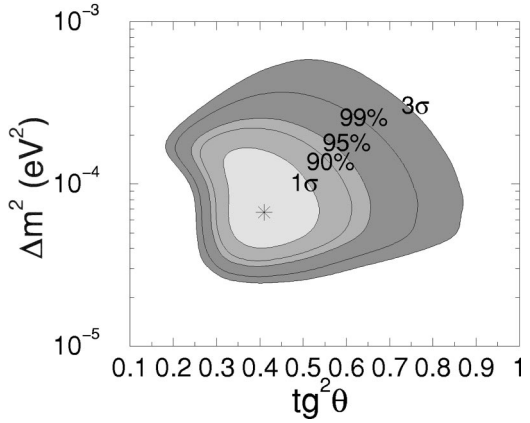


FIG. 4. Global LMA solution for $\sin^2\theta_{13}=0.04$. The boron neutrino flux is considered as a free parameter. The best fit point is marked by a star. The allowed regions are shown at $1\sigma$, 90% C.L., $2\sigma$, 99% C.L., and $3\sigma$.

### V. THREE NEUTRINO MIXING: EFFECT OF $\theta_{13}$

Results of the global analysis in the three neutrino context are shown in Fig. 4. To illustrate the effect of a third neutrino we use the three neutrino survival probability (5) for fixed value $\sin^2\theta_{13}=0.04$ near the upper bound from the CHOOZ experiment [34]. The number of degrees of freedom is the same as in the previous analysis.

We find the best fit point:

$$\Delta m^2_{12}=6.7\times10^{-5}\ \text{eV}^2,\quad \tan^2\theta=0.41,\quad f_B=1.09 \tag{21}$$

with $\chi^2=66.2$. The best fit value of $\Delta m^2_{12}$ is slightly higher than that in the two neutrino case, whereas the mixing angle is unchanged. The solution requires a slightly higher value of the boron neutrino flux. The changes are rather small, however, as a tendency, we find that with increase of $\theta_{13}$ the fit becomes worse in comparison with the $2\nu$ case. For $\sin^2\theta_{13}=0.04$ we get $\Delta\chi^2=1.0$.

In Fig. 4 we show the contours of a constant confidence level constructed with respect to the best fit point (21). The contours changed weakly for low mass values $\Delta m^2_{12}<10^{-4}$ eV$^2$ and there are significant changes for $\Delta m^2_{12}>10^{-4}$ eV$^2$. In particular, the $3\sigma$ upper bound on $\Delta m^2_{12}$ is $\Delta m^2_{12}<5.8\times10^{-4}$ eV$^2$; the lower $3\sigma$ bound on mixing: $\tan^2\theta_{12}=0.18$ (compare with numbers in Table I). Notice, however, that changes are substantially weaker if the contours are constructed with respect to the absolute minimum for $\theta_{13}=0$ (6).

The changes can be easily understood from the following analytical consideration.

The contribution of the last term in the probability (5) is negligible: for the largest possible value of $\theta_{13}$ it is below 0.5%. So, we can safely use approximation:

$$P_{ee}\approx\cos^4\theta_{13}P^{(2)}_{ee}\approx(1-2\sin^2\theta_{13})P^{(2)}_{ee}. \tag{22}$$

Mainly the effect of $\theta_{13}$ is reduced to the overall suppression of the survival probability. The suppression factor can be as small as 0.90–0.92.

In the fit with the free boron neutrino flux, the observables at high energies ($>5$ MeV) are determined by the following reduced rates

$$[\text{NC}]\equiv\frac{\text{NC}}{\text{NC}^{\text{SSM}}}=f_B,$$

$$[\text{CC}]\equiv\frac{\text{CC}}{\text{CC}^{\text{SSM}}}=f_B\cos^4\theta_{13}P^{(2)}_{ee},$$

$$[\text{ES}]\equiv\frac{\text{ES}}{\text{ES}^{\text{SSM}}}=f_B[\cos^4\theta_{13}P^{(2)}_{ee}(1-r)+r]. \tag{23}$$

As far as the fit of experimental data on CC events are concerned (SNO, SK, and partly, Homestake), the effects of $\theta_{13}$ is simply reduced to renormalization of the boron neutrino flux:

$$f_B\to\frac{f_B}{\cos^4\theta_{13}} \tag{24}$$

without change of the oscillation parameters $\Delta m_{12}$ and $\theta_{12}$. The dependence of the parameters on $\theta_{13}$ appears via the ratios of rates, which do not depend on $f_B$. From Eq. (23) we find

$$\cos^4\theta_{13}\frac{[\text{NC}]}{[\text{CC}]}\approx\frac{1}{P^{(2)}_{ee}} \tag{25}$$

$$\frac{\cos^4\theta_{13}}{r}\left[\frac{[\text{ES}]}{[\text{CC}]}-(1-r)\right]\approx\frac{1}{P^{(2)}_{ee}}. \tag{26}$$

So, the effect of $\theta_{13}$ is equivalent to a decrease of the ratios [NC]/[CC] and [ES]/[CC]. According to Fig. 4, this shifts the allowed regions to larger $\Delta m_{12}$ and $\theta_{12}$.

For low energy measurements (gallium experiments), sensitive to the $pp$-neutrino flux, which is known rather well, the increase of $\theta_{13}$ should be compensated by increase of the survival probability. This may occur due to increase of $\Delta m_{12}$ or/and decrease of $\tan^2\theta_{12}$.

For $\Delta m^2_{12}<10^{-4}$ eV$^2$ the boron neutrino spectrum is in the bottom of the suppression pit and the low energy neutrinos are on the adiabatic edge. In the fit, the increase of $\theta_{13}$ is compensated by the increase of $f_B$ and $\Delta m^2_{12}$. For $\Delta m^2_{12}>10^{-4}$ eV$^2$, the spectrum is in the region where conversion is determined mainly by averaged vacuum oscillations with some matter corrections: $P^{(2)}_{ee}\sim(1-0.5\sin^2 2\theta_{12})$. The dependence on $\Delta m^2_{12}$ is very weak which explains substantial enlargement of the allowed region to large values of $\Delta m^2_{12}$. The effect of $\theta_{13}$ can be compensated by decrease of $\theta_{12}$ which explains expansion of the region toward smaller $\tan^2\theta_{12}$.

For LOW solution increase of $\theta_{13}$ leads to improvement of the fit, so that this solution appears (for $\sin^2\theta_{13}=0.4$) at

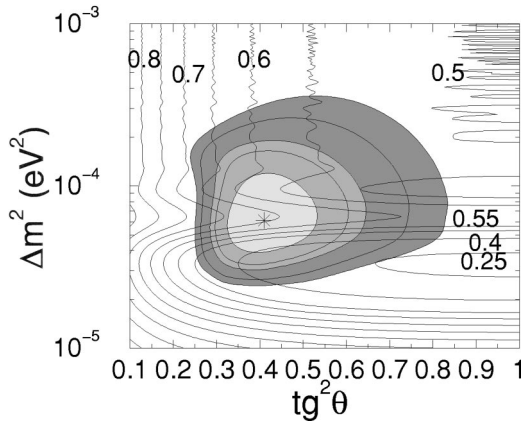


FIG. 5. Lines of constant total suppression at KamLAND. In the best fit point: $R_{\mathrm{Kam}}=0.65$.

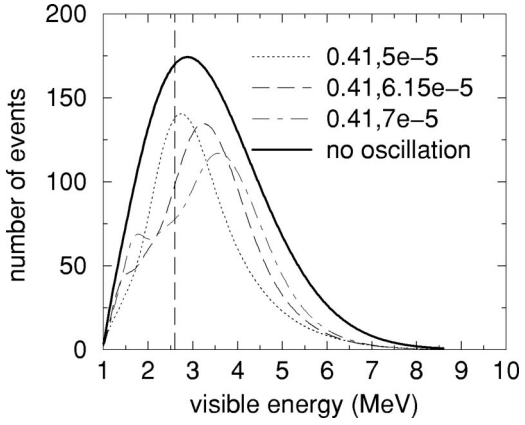


FIG. 6. Spectral distortion for three different values on $\Delta m^2$, including the best fit point of our analysis.

the $3\sigma$ level with respect to best fit point (21). Also for the SMA solution the effect of $\theta_{13}$ leads to slight improvement of the fit.

## VI. PREDICTIONS FOR KAMLAND

The next step in developments will be probably related to operation of the KamLAND experiment [38]. Both the total rate of events above the effective threshold $T_{eff}$ and the energy spectrum of events will be measured.

We characterize the effect of the oscillation disappearance by the ratio of the total number of events with visible energy above $T_{eff}$:

$$R_{\mathrm{Kam}}=\frac{1}{N_0}\int_{T_{eff}}\int_{T'}\int_{E} dE dT' dT \sum F_i P_i \frac{d\sigma}{dT} f(T,T'), \tag{27}$$

where $F_i$ is the flux from the $i$ reactor, $P_i$ is the survival probability for neutrinos from the $i$ reactor, $\sigma$ is the cross section of the detection reaction, and $f(T,T')$ is the energy resolution. $N_0$ is the rate without oscillations ($P_i=1$).

In our calculations we used the energy spectra of reactor neutrinos from [39,40]. The differential cross section of the $p+\overline{\nu}_e \rightarrow n+e^+$ reaction is taken from [41]. The parameters of the 16 nuclear reactors, maximal thermal power, distance from the reactor to the detector, etc., are given in [38]. We used the Gaussian form for the energy resolution function $f(T,T')$ with $\sigma/E=5\%/\sqrt{E(\mathrm{MeV})}$, and $T_{eff}=2.6$ MeV as the threshold for the visible energy [42].

In Fig. 5 we show the contours of the constant suppression factor in the $\Delta m^2-\tan^2\theta$ plot. In the best fit point

$$R_{\mathrm{Kam}}=0.65, \tag{28}$$

and in the $1\sigma$ region: $R_{\mathrm{Kam}}=0.4$–$0.7$.

Notice that the best fit point is in the range of lowest sensitivity of the total rate on $\tan^2\theta$. If, e.g., $R_{\mathrm{Kam}}$ is measured with 8% accuracy which would correspond to $R_{\mathrm{Kam}}=0.65\pm0.05$, we get from Fig. 5 that any mixing in the interval $\tan^2\theta=0.12$–$1.0$ is allowed.

The suppression factor strongly depends on $\Delta m^2$ in the range below the best fit point and this dependence is very weak for $\Delta m^2>10^{-4}$ eV$^2$. No bound on $\Delta m^2$ from the allowed region can be obtained by measurements of the total rate.

The distortion of the visible energy spectrum depends on $\Delta m^2$ strongly. In Fig. 6 we show the spectrum for different values of $\Delta m^2$. There is a shift of maximum to large $E$ with increase of $\Delta m^2$. For the best fit value of $\Delta m^2$ the maximum is at $E\approx3.5$ MeV. The most profound effect of oscillations is the suppression of rate at high energies. For instance, for $E\approx5$ MeV the suppression factor is smaller than 1/2.

## VII. CONCLUSIONS

We find that the LMA MSW solution with parameters $\Delta m^2\sim6.15\times10^{-5}$ eV$^2$ and $\tan^2\theta=0.41$ gives the best fit to the data. The solution reproduces well the zenith spectrum measured by SK and the day and night spectra at SNO. It is in a very good agreement with SSM flux of the boron neutrino: $f_B=1.05$.

The recent SNO results together with zenith spectra results from SK slightly shifted the best fit point to larger $\Delta m^2$ and $\theta$. At the same time the allowed regions of oscillation parameters shrunk, leading to important, and statistically significant, upper bounds on mixing angle and $\Delta m^2$. Now we have strong evidence that ''solar'' mixing is nonmaximal, and moreover, deviation from maximal mixing is rather large. We find that quasivacuum oscillation solution with $\Delta m^2=4.5\times10^{-10}$ eV$^2$ and mixing in the dark side is the only other solution accepted at $3\sigma$ level, provided that the boron neutrino flux is about 30% below the SSM value.

The LOW solution is accepted at slightly higher than the $3\sigma$ level and it reappears at the $3\sigma$ level if $\theta_{13}$ is included.

The SMA solution gives very bad fit of the data especially the SNO spectra predicting a rather small contribution of the NC events in comparison with CC events.

We find that $\theta_{13}$ produces a rather small effect on the solutions even with new high statistics data. As a tendency we see that inclusion of the $\theta_{13}$ effect worsens the fit of the data in the LMA region, and shifts the best fit point to larger $\Delta m^2_{12}$.

We have found predictions for the KamLAND experiment: in the best fit point one expects the suppression factor for total signal $\sim 0.6$ to 0.7 and the spectrum distortion with substantial suppression in the high energy part.

*Note added*. This section has been added up on request of the referee to perform critical comparison of existing results from global analyses of the data including results of papers which have appeared *after* our publication [43–45].


## ACKNOWLEDGMENT

We thank Professor Mark Chen for clarification of the way SNO treats the correlations between the systematic uncertainties. The authors are grateful to J. N. Bahcall for emphasizing the necessity to take into account correlations of cross-section uncertainties in contributions of different fluxes to Ar and Ge production rates we have discussed in Sec. II D.


## APPENDIX

The systematic uncertainties were treated according to [23]. Writing the total counting rate in SNO as a sum over different contributions and different spectral bins, we have:

$$R_j = \sum_{i=1,5} R_{ij}, \tag{A1}$$

where the index $j$ stands for the different spectral bins and $i$ runs over the five contributions to the SNO data (CC, NC, ES, neutron background, and low energy background). We assume that all systematic uncertainties of the SNO result are the uncertainties in the theoretical prediction. These uncertainties can be written in terms of the systematic uncertainties of the input parameters of experiment ($X_k$):

$$\sigma^2_{j_1,j_2}(TH) = \sum_{k=1,14} \frac{\partial R_{j_1}}{\partial \ln X_k} \frac{\partial R_{j_2}}{\partial \ln X_k} (\Delta \ln X_k)^2. \tag{A2}$$

We take the systematic uncertainties from [5]. The different systematic uncertainties are added in quadrature.

Equation (A2) can be written in terms of the different contributions $R_{ij}$ (A1) as

$$\sigma^2_{j_1,j_2}(TH) = \sum_{i_1=1,5} \sum_{i_2=1,5} R_{i_1 j_1} R_{i_2 j_2} \sum_{k=1,14} \alpha_{i_1,j_1,k} \alpha_{i_2,j_2,k} (\Delta \ln X_k)^2, \tag{A3}$$

where we have introduced the parameters $\alpha_{i,j,k}$:

$$\alpha_{i,j,k} \equiv \frac{\partial \ln R_{i,j}}{\partial \ln X_k}. \tag{A4}$$

These parameters are numerically estimated by changing the response function of the detector through changes in the parameters $X_k$.

There is a qualitative agreement between results of different groups in that the LMA solution gives the best fit, the LOW and VO solutions have comparable goodnesses of the fit and appear at about $3\sigma$ level with respect to the global minimum, the SMA solution is strongly disfavored. At the same time, there is a rather significant *quantitative* difference of results. (Some of these differences have already been marked in the paper.)

In general, the difference in results can be related to the following ingredients.

(1) Input data. Super-Kamiokande: The majority of groups used the zenith spectra. The day–night spectra have been used by Barger *et al.*, and by the SNO collaboration. This can partly explain the significant difference of their results.

Gallium experiments: The data have been analyzed in three different ways: (i) combining rates from Gallex and GNO and using the SAGE rate as an independent measurement, (ii) combining all three rates [19,20], and (iii) using combined rates and the seasonal asymmetry [44]. In the present paper as well as in [43–45] the new GNO data published at Neutrino 2002 have been included.

SNO: the data have been used following prescriptions of collaboration. However, we can not reproduce exactly results of analysis of SNO data by the SNO collaboration [4] itself. The allowed LMA regions from our analysis is shifted to larger mixing angles. Similar shift has been found by Fogli *et al.* [44].

(2) Solar neutrino fluxes. There are different treatments of the boron neutrino flux: in [19] and in the present paper $f_B$ was taken as a free parameter, whereas the SSM predictions have been used in [44,45]. The *hep*-neutrino flux is either ignored or used according to prescription in [19] without error.

(3) Method. Treatment of errors. Substantial differences can be related to correlations of errors, and propagation of systematic and theoretical errors to the observables.

(4) Conversion and oscillation probabilities. In principle, there is no ambiguity or inaccuracy in calculations of probabilities. Still some features of results may testify for the difference in the description of Earth regeneration effect.

Let us now compare results of different groups, concentrating on the points, where disagreement is significant.

(1) There is a large spread of values of $\chi^2_{\rm min}$(LMA) in the LMA region which cannot be explained by the difference of numbers of degrees of freedom used: e.g., Maltoni *et al.*: $\chi^2_{\rm min}(\mathrm{LMA}) = 66.1$ (79 DOF), this paper: $\chi^2_{\rm min}(\mathrm{LNA}) = 65.2$ (78 DOF), Bahcall *et al.*: $\chi^2_{\rm min}(\mathrm{LMA}) = 75.4$ (77 DOF). The difference $\Delta\chi^2 = 9.3 - 10.2$ cannot be explained by distortion of the spectrum which could enhance inaccuracies.

The spread of the oscillation parameters in the best fit points from the latest analyses is reasonably small and stable.

A stronger difference appears in the contours of constant confidence level (C.L.) far from the best fit point. In particular, there is substantial difference in C.L. at which maximal mixing is accepted, or the difference of $3\sigma$ upper bounds on mixing angle: $\tan^2\theta_{\rm max} = 0.55$ (SNO), 0.64 (Barger *et al.*), 0.89 (Bahcall *et al.*), 0.84 (this paper), 0.83 (Maltoni *et al.*), 1.0 (Fogli *et al.*). Also the difference appears in the maximal allowed value of $\Delta m^2$ allowed at a given C.L. For instance,

at the $3\sigma$ level we get from different analyses in the units of $10^{-4}$ eV$^2$: $\Delta m^2_{\rm max}=1.9$ (SNO), 2.3 (Barger *et al.*), 3.4 (this paper), 3.7 (Bahcall *et al.*), 8 (Fogli *et al.*), 10 (Maltoni *et al.*).

Thus the shapes of the function $\chi^2=\chi^2(\Delta m^2,\tan^2\theta)$ found by different groups differ substantially even in the LMA region.

(2) In the LOW region the spread of $\Delta\chi^2_{\rm min}({\rm LOW\text{-}LMA})\equiv\chi^2_{\rm min}({\rm LOW})-\chi^2_{\rm min}({\rm LMA})$ is relatively small: $\Delta\chi^2_{\rm min}({\rm LOW\text{-}LMA})=9.3$–$12.4$. It is smaller than the spread of absolute values of $\chi^2_{\rm min}({\rm LOW})$. So, the global minimum (in LMA) and the local one in the LOW region shift simultaneously. Also the spread of oscillation parameters in the best fit points of the LOW solution is small.

The situation is similar for the VO solution: the spread of $\Delta\chi^2_{\rm min}({\rm VO\text{-}LMA})\sim 8$–$10$ is relatively small with the exception of results of Barger *et al.*, and, to some extent, Bandyopadhyay *et al.*

(3) There is a large spread of $\Delta\chi^2_{\rm min}({\rm SMA\text{-}LMA})\equiv\chi^2_{\rm min}({\rm SMA})-\chi^2_{\rm min}({\rm LMA})$ obtained by different groups in the SMA region. The result of our analysis is rather close to the one performed by Bandyopadhyay *et al.*: $\Delta\chi^2=\chi^2_{\rm min}({\rm SMA})-\chi^2_{\rm min}({\rm LMA})\sim 31$–$34$. The analysis made by Barger *et al.*, disfavors SMA much stronger: $\Delta\chi^2_{\rm min}({\rm SMA\text{-}LMA})=57.3$. On the other hand, the analyses by Bahcall *et al.*, Fogli *et. al.*, and Maltoni *et al.*, give rather close values $\Delta\chi^2_{\rm min}({\rm SMA\text{-}LMA})\sim 23$–$26$ which are about 9 to 10 smaller than in the present paper. Moreover, the position of minimum in the oscillation parameter plane is different (see Sec. IV C).

In this connection the following remarks are in order.

There is no significant difference in $\chi^2_{\rm min}$ in the SMA region: $\chi^2_{\rm min}=101$ (Bahcall *et al.*), $\chi^2=99.7$ (this paper) $\chi^2_{\rm min}=96.9$ (Fogli *et al.*), $\chi^2=99.5$ (Bandyopadhyay *et al.*). So, the spread of differences $\Delta\chi^2_{\rm min}$(SMA-LMA) obtained by different groups is not because of the difference in $\chi^2_{\rm min}$(SMA), but, mainly, because of spread in $\chi^2_{\rm min}$(LMA).

The possible difference in results can be due to various treatments of the systematic errors and their propagation to observables. In particular, the uncertainty in the absolute scale of the neutrino energy propagates to the errors in the individual energy bins in a way which depends on the distortion of the energy spectrum. This, however, should not affect solutions with flat spectrum distortion, like LMA or LOW, and SMA with very small mixing.

It is expected that far from the favored region (region of global minimum of $\chi^2$) the functions $\chi^2(\Delta m^2,\tan^2\theta)$ obtained from different analyses can be substantially different (accumulation of errors, instability of the analysis, etc.). However, the comparison performed above does not support this expectation completely: significant spread of $\chi^2$ appears already in the global minimum.

Clearly, the difference $\Delta\chi^2\sim 3-5$ from complicated analysis with many degrees of freedom should not be considered as a problem. The spread $\Delta\chi^2\sim 10$ is on the borderline. It does not yet change the implications of results. Most probably the spread originates from different treatments of the systematic correlated errors. Larger values of $\Delta\chi^2$ can be really problematic: they may lead to different interpretations of results.


[1] SNO Collaboration, Q. R. Ahmad *et al.*, Phys. Rev. Lett. **87**, 071301 (2001).

[2] A. B. McDonald, in *Proceedings of the 19th International Conference on Neutrino Physics and Astrophysics, Neutrino 2000*, Sudbury, Canada 2000 [Nucl. Phys. B (Proc. Suppl.) **91**, 21 (2001)].

[3] SNO Collaboration, Q. R. Ahmad *et al.*, Phys. Rev. Lett. **89**, 011301 (2002).

[4] SNO Collaboration, Q. R. Ahmad *et al.*, Phys. Rev. Lett. **89**, 011302 (2002).

[5] "How to use the SNO Solar Neutrino Spectral Data," at http://www.sno.phy.queensu.ca/

[6] Super-Kamiokande Collaboration S. Fukuda *et al.*, Phys. Rev. Lett. **86**, 5651 (2001); **86**, 5656 (2001).

[7] M. B. Smy, in *Proceedings of 3rd Workshop on Neutrino Oscillations and Their Origin (NOON, 2001)*, Kashiwa, Japan, 2001, edited by Y. Suzuki, M. Nakahata, Y. Fukuda, Y. Takeuchi, T. Mori, and T. Yoshida (World Scientific, Singapore, 2002); hep-ex/0202020.

[8] M. B. Smy, in *Proceedings of NO-VE International Workshop on Neutrino Oscillations in Venice*, Venice, Italy, 2001, edited by M. Baldo Ceolin, hep-ex/0108053.

[9] J. N. Bahcall, P. I. Krastev, and A. Yu. Smirnov, Phys. Rev. D **62**, 093004 (2000); **63**, 053012 (2001).

[10] J. N. Bahcall, P. I. Krastev, and A. Yu. Smirnov, J. High Energy Phys. **5**, 15 (2001).

[11] V. Barger, D. Marfatia, and K. Whisnant, Phys. Rev. Lett. **88**, 011302 (2002).

[12] G. L. Fogli, E. Lisi, D. Montanino, and A. Palazzo, Phys. Rev. D **64**, 093007 (2001); hep-ph/0203138.

[13] J. N. Bahcall, M. C. Gonzalez-Garcia, and Carlos Peña-Garay, J. High Energy Phys. **08**, 014 (2001); **04**, 007 (2002).

[14] A. Bandyopadhyay, S. Choubey, S. Goswami, and K. Kar, Phys. Lett. B **519**, 83 (2001).

[15] P. I. Krastev and A. Yu. Smirnov, Phys. Rev. D **65**, 073022 (2002).

[16] A. M. Gago *et al.*, Phys. Rev. D **65**, 073012 (2002).

[17] P. Aliani, V. Antonelli, M. Picariello, and E. Torrente-Lujan, Nucl. Phys. **B634**, 393 (2002).

[18] V. Barger, D. Marfatia, K. Whisnant, and B. P. Wood, Phys. Lett. B **537**, 179 (2002).

[19] J. N. Bahcall, M. C. Gonzalez-Garcia, and C. Peña-Garay, J. High Energy Phys. **07**, 054 (2002).

[20] A. Bandyopadhyay, S. Choubey, S. Goswami, and D. P. Roy, Phys. Lett. B **540**, 14 (2002).

[21] P. Creminelli, G. Signorelli, and A. Strumia, J. High Energy Phys. **05**, 852 (2001).

[22] P. Aliani *et al.*, hep-ph/0205053.

[23] G. L. Fogli and E. Lisi, Astropart. Phys. **3**, 185 (1995).
[24] B. T. Cleveland *et al.*, Astrophys. J. **496**, 505 (1998); K. Lande *et al.*, in *Neutrino 2000* [2] [Nucl. Phys. B (Proc. Suppl.) **91**, 50 (2001)].
[25] SAGE Collaboration, J. N. Abdurashitov *et al.*, J. Exp. Theor. Phys. **95**, 181 (2002) [Zh. Eksp. Teor. Fiz. **122**, 211 (2002)].
[26] C. M. Cattadori *et al.*, in Proceedings of the TAUP 2001 Workshop, Gran-Sasso, Assesrgi, Italy.
[27] Mark Chen (private communication).
[28] J. N. Bahcall, M. H. Pinsonneault, and S. Basu, Astrophys. J. **555**, 990 (2001).
[29] L. E. Marcucci *et al.*, Phys. Rev. C **63**, 015801 (2001); T.-S. Park *et al.*, nucl-th/0107012, and references therein.
[30] G. L. Fogli, E. Lisi, D. Montanino, and A. Palazzo, Phys. Rev. D **62**, 013002 (2000).
[31] A. Bandyopadhyay, S. Choubey, S. Goswami, and K. Kar, Phys. Rev. D **65**, 073031 (2002).
[32] J. N. Bahcall, M. C. Gonzalez-Garcia, and C. Peña-Garay, Phys. Rev. C **66**, 035802 (2002).
[33] J. N. Bahcall, P. I. Krastev, and A. Yu. Smirnov, Phys. Rev. D **60**, 093001 (1999).
[34] CHOOZ Collaboration, M. Apollonio *et al.*, Phys. Lett. B **420**, 397 (1998).
[35] M. C. Gonzalez-Garcia, C. Peña-Garay, Y. Nir, and A. Yu. Smirnov, Phys. Rev. D **63**, 013007 (2001).
[36] S. P. Mikheyev and A. Yu. Smirnov, *'86 Massive Neutrinos in Astrophysics and in Particle Physics, Proceedings of the 6th Moriond Workshop*, edited by O. Fackler and J. Tran Thanh Van (Edition Frontières, Gif-sur-Yvette, 1986), p. 355; A. J. Baltz and J. Weneser, Phys. Rev. D **50**, 5971 (1994); **51**, 3960 (1994); E. Lisi and D. Montanino, *ibid.* **56**, 1792 (1997); J. M. Gelb, W. Kwong, and S. P. Rosen, Phys. Rev. Lett. **78**, 2296 (1997).
[37] S. T. Petcov, Phys. Lett. B **434**, 321 (1998); E. Kh. Akhmedov, Nucl. Phys. **B538**, 25 (1999); M. V. Chizhov and S. T. Petcov, Phys. Rev. Lett. **83**, 1096 (1999); E. Kh. Akhmedov and A. Yu. Smirnov, *ibid.* **85**, 3978 (2000).
[38] J. Busenitz *et al*, ''Proposal for US Participation in KamLAND,'' March 1999, downloadable at http://bfk1.lbl.gov/kamland/
[39] P. Vogel and J. Engel, Phys. Rev. D **39**, 3378 (1989).
[40] H. Murayama and A. Pierce, Phys. Rev. D **65**, 013012 (2002).
[41] P. Vogel and J. F. Beacom, Phys. Rev. D **60**, 053003 (1999).
[42] J. Shirai, talk given at Neutrino 2002 (unpublished).
[43] A. Strumia, C. Cattadori, N. Ferrari, and F. Vissani, Phys. Lett. B **541**, 327 (2002).
[44] G. L. Fogli, E. Lisi, A. Marrone, D. Montanino, and A. Palazzo, Phys. Rev. D **66**, 053010 (2002).
[45] M. Maltoni, T. Schwetz, M. A. Tortola, and J. W. F. Valle, hep-ph/0207227.